Published in final edited form as:
Virology. 2012 December 5; 434(1): 18–26. doi:10.1016/j.virol.2012.07.020.

A replication-deficient rabies virus vaccine expressing Ebola virus glycoprotein is highly attenuated for neurovirulence

Amy B. Papaneri[a], **Christoph Wirblich**[b], **Jennifer A. Cann**[c], **Kurt Cooper**[c], **Peter B. Jahrling**[a,c], **Matthias J. Schnell**[b,d], and **Joseph E. Blaney**[a]

[a]Emerging Viral Pathogens Section, National Institute of Allergy and Infectious Diseases, National Institutes of Health, Fort Detrick MD, 21702 USA

[b]Department of Microbiology and Immunology, Jefferson Medical College, Thomas Jefferson University, Philadelphia PA, 19107 USA

[c]Integrated Research Facility, National Institute of Allergy and Infectious Diseases, National Institutes of Health, Fort Detrick MD, 21702 USA

[d]Department of Jefferson Vaccine Center, Jefferson Medical College, Thomas Jefferson University, Philadelphia PA, 19107 USA

Abstract

We are developing inactivated and live-attenuated rabies virus (RABV) vaccines expressing Ebola virus (EBOV) glycoprotein for use in humans and endangered wildlife, respectively. Here, we further characterize the pathogenesis of the live-attenuated RABV/EBOV vaccine candidates in mice in an effort to define their growth properties and potential for safety. RABV vaccines expressing GP (RV-GP) or a replication-deficient derivative with a deletion of the RABV G gene (RVΔG-GP) are both avirulent after intracerebral inoculation of adult mice. Furthermore, RVΔG-GP is completely avirulent upon intracerebral inoculation of suckling mice unlike parental RABV vaccine or RV-GP. Analysis of RVΔG-GP in the brain by quantitative PCR, determination of virus titer, and immunohistochemistry indicated greatly restricted virus replication. In summary, our findings indicate that RV-GP retains the attenuation phenotype of the live-attenuated RABV vaccine, and RVΔG-GP would appear to be an even safer alternative for use in wildlife or consideration for human use.

Keywords

Ebola virus; rabies virus; vaccine; neurovirulence; mice

Introduction

Several viruses from the *Ebolavirus* genus and *Marburgvirus* genus, Family *Filoviridae*, cause severe and often fatal viral hemorrhagic fever in humans and nonhuman primates

Corresponding Authors: J. Blaney, EVPS, NIAID, NIH, Integrated Research Facility, 8200 Research Plaza, Fort Detrick MD 21702, phone: 301-631-7211, Fax: 301-619-5029, jblaney@niaid.nih.gov, M. Schnell, Dept. of Microbiology and Immunology, Jefferson Medical College, Thomas Jefferson University, 233 South 10th St, 531 BLSB, Philadelphia PA 19107, phone: 215-503-4634, Fax: 215-503-5393, matthias.schnell@jefferson.edu.

(Sanchez et al., 2007). The high case fatality rate, public health threat in Africa, and biodefense concerns associated with these viruses have resulted in considerable effort and progress in filovirus vaccine development (Bradfute et al., 2011; Geisbert et al., 2010). Several vaccination strategies have been developed that confer protection in animal models, but issues of safety, preexisting vector immunity, production, or lack of commercial interest have slowed progress (Bukreyev et al., 2010; Geisbert et al., 2010; Hensley et al., 2010; Sun et al., 2009; Warfield et al., 2007). An Ebola virus (EBOV) vaccine would be directed for use in humans at risk of infection in Africa as well as for healthcare providers, first responders, soldiers, or travelers. A second application for EBOV vaccines would be utilization in endangered wildlife at risk of lethal EBOV disease including gorillas and chimpanzees of Central Africa. Studies have indicated that EBOV outbreaks have resulted in numerous nonhuman primate (NHP) deaths in Gabon and the Republic of Congo, which could hinder conservation efforts (Bermejo et al., 2006; Leroy et al., 2004; Rouquet et al., 2005). A vaccine to protect these at risk animals would have a second critical benefit to humans. As EBOV is a zoonotic disease with documented human outbreaks arising from contact with diseased nonhuman primates (NHPs) (Mahanty and Bray, 2004), prevention of disease in NHPs might reduce the frequency of transmission to humans.

We sought to identify a vaccine platform for EBOV and other filoviruses of public health importance that would result in promising candidates for use in both humans and endangered wildlife. To this end, we have developed (a) replication-competent, (b) replication-deficient, and (c) chemically inactivated rabies virus (RABV) vaccines expressing EBOV (Zaire; Mayinga) glycoprotein (GP) (Blaney et al., 2011). The recombinant RABV vaccine platform has been used to generate vaccine candidates for several viral pathogens and is characterized by strong replication, potent induction of humoral and cellular immunity, and genetic stability of inserts (Gomme et al., 2011; Mebatsion et al., 1996). Our primary focus is the development of an inactivated vaccine for use in humans based on the potential for superior safety and the successful history of the existing beta propiolactone-inactivated RABV vaccine that is widely used in humans. As RABV is still a considerable public health issue in Africa with an estimated 24,000 deaths reported yearly (Cleaveland et al., 2002; Knobel et al., 2002; Schnell et al., 2010), a bivalent vaccine that confers protection from RABV and EBOV would be an economical and efficient public health tool. However, in addition to the development of inactivated RABV/EBOV vaccines, the parental recombinant RABV vaccine used to generate the RABV/EBOV vaccine candidates is derived from the SAD B19 strain, which is used for wildlife vaccination by baiting in Europe suggesting additional applications of our vaccine candidates (Vos et al., 1999; Vos et al., 2002). Therefore, live-attenuated RABV/EBOV vaccines could be considered for use in Africa in an analogous campaign to protect at risk NHPs from lethal EBOV infections.

Here, our goal was to further define the virological properties and virulence of the replication competent, RV-GP, and replication deficient, RVΔG-GP, vaccine candidates that we have previously described (Blaney et al., 2011). Both RV-GP and RVΔG-GP, which has a deletion removing the entire RABV glycoprotein (G) gene, were found to be avirulent upon peripheral administration in mice. Each bivalent vaccine candidate induced strong humoral immunity to RABV G and EBOV GP, and conferred protection from both lethal RABV and mouse-adapted (MA) EBOV challenge in mice (Blaney et al., 2011). Here we further characterize the high degree of attenuation of these vaccine candidates in comparison to the existing parental live-attenuated RABV vaccine already used in wildlife.

Results

RABV vaccine vectored EBOV GP vaccine candidates and their replication in cell culture

The construction and propagation of the recombinant vaccine viruses studied here has been previously described. The parental RABV vaccine vector, RVA(p), is a recombinant derivative of the SAD B19 RABV vaccine strain, which has been used as a live oral vaccine for wildlife in Europe (Figure 1) (McGettigan et al., 2003). RVA, a further attenuated vaccine vector containing an Arg→Glu change at amino acid 333 of RABV G, was used to generate RVGP, which expresses EBOV Mayinga glycoprotein (GP) (Blaney et al., 2011). RVΔG-GP expresses EBOV Mayinga GP but contains a deletion of the RABV G gene requiring propagation on *trans*-complementing BSR-G cells (Blaney et al., 2011).

We first sought to determine the effect of EBOV GP expression on replication of the RABV vaccines in cell culture. Robust replication in appropriate cell culture is critical to the development of a cost-effective vaccination strategy. Here we present the optimal conditions for replication of RV-GP and RVΔG-GP. We first evaluated the replication of the vaccine viruses in Vero cells (Figure 2A), which are a cell line currently in use for the production of human vaccines. At a multiplicity of infection (m.o.i.) of 5, RV-GP reached a virus titer of 8.0 Log_{10}FFU/ml at five days post-infection. Importantly, the expression of EBOV GP does not appear to decrease the virus production when the vectored viruses are compared to levels reached by the control RABV viruses, RVA(p) or RVA. We also assessed the replication of the RABV G deletion virus, RVΔG-GP, in (A) Vero cells and (B) BSR-G cells. As expected due to its design as a replication-deficient virus, RVΔG-GP did not replicate in Vero cells (Figure 2A). In contrast, RVΔG-GP reached virus titers of 7.4 Log_{10}FFU/ml in BSR-G cells expressing RABV G (Figure 2B). These results confirm the restricted growth properties of RVΔG-GP but indicate that the vaccine candidate can be propagated to high levels under appropriate conditions (e.g. trans-complementing cells) demonstrating that each vaccine candidate replicates to levels suitable for production with little effort at optimization thus far.

Neuroinvasiveness in immunodeficient mice

Our previous results have indicated that peripheral injection of RABV vaccine viruses expressing GP (with or without RABV G) by the intramuscular (i.m.), intranasal (i.n.), or intraperitoneal (i.p.) route in immunocompetent mice resulted in no morbidity or moribundity (Blaney et al., 2011). Here, we next sought to further determine the safety profile of our vaccine candidates by peripheral administration to immunodeficient ICR-SCID mice (Figure 3). Groups of eight adult ICR-SCID mice were injected i.m. in the hind leg with vehicle (PBS) or $1x10^6$ FFU of RVA(p), RVA, RV-GP, or RVΔG-GP. Mice were monitored daily for signs of infection and survival for 84 days. Results indicated that 2 of 8 and 1 of 8 RVA(p)- and RVA-infected mice succumbed to infection, respectively. Similarly, 1 of 8 mice injected with RV-GP succumbed to infection. No mice in the vehicle (PBS) or RVΔG-GP groups succumbed to infection. These results indicated that GP expression did not increase the virulence of the parent RABV vaccine vector in mice without functional adaptive immunity, which is a further indication of the safety of these vaccine candidates. Furthermore, RVΔG-GP showed no virulence in immunodeficient mice.

Neurovirulence in adult and suckling mice

RVA(p) retains neurovirulence upon intracerebral (i.c.) infection of adult mice. However, RVA which was used to generate RV-GP is avirulent when administered by i.c. injection by virtue of the Arg→Glu change at amino acid 333 of RABV G (McGettigan et al., 2003). We sought to determine if expression of EBOV GP would modify neurovirulence in adult mice. Groups of eight four-week-old mice were injected i.c. with vehicle or $1x10^5$ FFU of

RVA(p), RVA, RV-GP, or RVΔG-GP, and monitored daily for survival (Figure 4). As expected, RVA(p) was lethal upon i.c. injection with 100% of mice succumbing by day 10. In contrast, 100% of mice inoculated with RVA, RV-GP and RVΔG-GP survived infection, and there was no evidence of any clinical signs. Thus, in adult mice, both RV-GP and RVΔG-GP lack neurovirulence.

In contrast to results observed in adult mice, both RVA(p) and RVA retain neurovirulence when administered to suckling mice by the i.c. route (Blaney et al., 2011). RVGP and RVΔG-GP were previously evaluated for neurovirulence by i.c. injection of suckling mice and RV-GP was also found to be lethal (Blaney et al., 2011). In contrast, RVΔG-GP was found to be avirulent in suckling mice injected i.c. at the highest dose tested, $6x10^4$ FFU. Here we sought to confirm and expand these results by administration of a higher dose, $1x10^5$ FFU, of RVΔG-GP in suckling mice by the i.c. route (Table 1). RVΔG-GP was again found to induce no disease in suckling mice. In contrast RVA was 100% lethal at 10^4 and 10^2 FFU while administration of 10^1 and 10^0 FFU resulted in 30% lethality and no lethality, respectively. The LD_{50} for RVA was determined to be 5.2 FFU while the LD_{50} for RVΔG-GP was $>10^5$ FFU. These results indicate that RVΔG-GP has at least a 19,000-fold reduction in neurovirulence compared to RVA as compared by LD_{50}.

Analysis of RVΔG-GP replication in suckling mouse brain

RVA and RV-GP lack neurovirulence in adult mice but retain it in suckling mice. In contrast, RVΔG-GP appears to lack neurovirulence in both adult and suckling mice. Therefore, we next attempted to compare the vaccine viruses for growth properties in suckling mouse brain and to determine if RVΔG-GP has any capacity for replication in the brain. Five-day-old Swiss Webster mice were inoculated i.c. with $1x10^5$ FFU of RVA(p), RVA, RVA-GP, or RVΔG-GP (Figure 5). On days 1, 3, 5, 6, 7, 9, 14, and 21, three surviving mice per group were euthanized, brain homogenates were generated, and levels of viral genomic RNA were determined by quantitative reverse transcription polymerase chain reaction (qRT-PCR) targeting the RABV N gene. As expected, viral load was highest in the RVA(p) group, peaking at nearly 10.0 Log_{10}genomic equivalents/μg of total RNA. Peak viral load of RVA and RV-GP were approximately 10-fold reduced and delayed when compared to RVA(p). As expected, no mice injected with these viruses survived past day 9. In contrast, mice injected with RVΔG-GP survived to study end and reached a peak viral genomic load in the brain at day 9 of approximately 7.0 Log_{10}genomic equivalents/μg of total RNA which is approximately 1,000-fold reduced from levels observed for RVA(p). These results indicate that although RVΔG-GP is avirulent upon i.c. injection of suckling mice, viral mRNA is expressed and/or the viral genome retains at least some capacity to amplify, persisting to at least day 21.

We next sought to determine if infectious virus could be recovered from the brains of RVΔG-GP-infected mice in comparison to RVA. Five-day-old Swiss Webster mice were inoculated i.c. with $1x10^5$ FFU of RVA or RVΔG-GP. On days 1, 3, 5, 7, 9, 14, 21, 28, 35, and 42, three surviving mice per group were euthanized, and brain homogenates were generated and assayed for focus formation on Vero cells and BSR-G cells (Figure 6). Analysis of RVA replication by titration of brain homogenates in Vero cells indicated that virus replication was robust as expected with mean peak virus titers reaching 9.3 Log_{10}FFU/ml. In contrast, when samples of RVΔG-GP were observed when brain homogenates were titrated in Vero cells, no detectable viral foci were observed. However, titration of brain homogenates in BSR-G cells demonstrated that RVΔG-GP did replicate in the brain to a mean peak virus titer of 4.7 Log_{10}FFU/ml, albeit at a greatly reduced level when compared to RVA (8.8 Log_{10}FFU/ml). For RVΔG-GP, infectious virus was detectable and peaked at day 7 followed by a reduction to undetectable virus levels by day 21. By comparison of

mean peak virus titer in BSR-G cells, RVΔG-GP appears to have an approximately 10,000-fold reduction in the ability to replicate in the brain when compared to RVA.

Histopathological and immunohistochemical analysis of RVΔG-GP replication in suckling mouse brain

Based on the indication of limited genomic and viral replication of RVΔG-GP in the brain, we next sought to compare the evidence of viral spread and resulting inflammation associated with RVA and RVΔG-GP infection using histopathological (H&E) and immunohistochemical (IHC) analysis. Five-day-old Swiss Webster mice were inoculated i.c. with $1x10^5$ FFU of RVA and RVΔG-GP. On days 1, 3, 5, 7, 9, 14, and 21, three surviving mice per group were euthanized and brains were processed for H&E or IHC analysis as described in the Materials and Methods. Inflammation and anti-RABV immunohistochemical staining were semi-quantitatively scored in the cerebellum and hippocampus in each of three brains per group using a 0–3 scale (0 = none, 1 = mild, 2 = moderate, and 3 = severe). Mean severity scores for meningoencephalitis and antigen staining in RVA- and RVΔG-GP-infected brains are summarized in Figure 7. Inflammation in the cerebellum and hippocampus of RVA-infected brains peaked on days 5 to 9 reaching mean scores of 2.5 to 3.0, while RVΔG-GP-infected brains had more constant scores ranging from approximately 0.5 to 1.5 during the 3 week study. Analysis of the presence of viral antigen also indicated that staining peaked in the cerebellum and hippocampus of RVA-infected brains on day 5, 7, and 9 although hippocampal antigen staining was more pronounced with scores ranging from 2.0 to 3.0. Analysis of RVΔG-GP- infected brains did not appear to demonstrate evidence of viral spread as antigen staining was consistently low throughout the study ranging from 0.0 to 1.3.

In the cerebellum of RVA-infected mice, the cortical cerebellar architecture became progressively disrupted by a moderate to markedly dense inflammatory infiltrate composed primarily of neutrophils (Figure 8). The infiltrate was most dense within the granule cell and Purkinje cell layers, and extended to a lesser extent into the molecular and outer granular cell layers as well as the meninges. Anti-RABV immunohistochemistry revealed abundant cytoplasmic staining within inflammatory cells and neurons. In contrast, the cerebellar architecture remained intact in RVΔG-GP-infected brains. Minimal to mild neutrophilic and lymphocytic inflammation was found in most animals; in two individuals the degree of inflammation was classified as moderate. Anti-RABV immunohistochemistry revealed either no staining or occasional staining within inflammatory cells or neurons.

Analysis of the hippocampus from RVA-infected brains indicated that over the course of the study, the hippocampal architecture became progressively disrupted by a moderate to markedly dense inflammatory infiltrate composed primarily of neutrophils and lymphocytes (Figure 9). The destruction was most marked within the CA3, CA4, and dentate gyrus regions of the hippocampus. Anti-RABV immunohistochemistry revealed discrete cytoplasmic staining within large numbers of inflammatory cells, most commonly neutrophils, and to a lesser extent, within neurons. In RVΔG-GP-infected brains, the hippocampal architecture remained intact. Occasionally, diffusely distributed neutrophils and lymphocytes were seen, but the overall degree of inflammation was minimal to mild. Anti-RV immunohistochemistry revealed either no staining or occasional staining within isolated inflammatory cells or neurons.

Discussion

In addition to the demonstration of immunogenicity and clinical efficacy for a live virus vaccine candidate, the demonstration of vaccine safety and knowledge of the virological properties of live vaccines is paramount. For live vaccines that may cause disease of the

central nervous system (CNS), two parameters that define neurotropic viral pathogenesis require investigation, neuroinvasiveness and neurovirulence. Neuroinvasiveness describes the ability of a virus to invade the CNS when inoculated at a peripheral site, while neurovirulence describes the capacity of a virus to induce disease when administered directly into the brain. While live RABV vaccine vectors have previously been used as a safe and efficacious platform to generate vaccine candidates against several pathogens (Faber et al., 2005; Faul et al., 2009; McGettigan et al., 2003; Mustafa et al., 2011; Siler et al., 2002), we sought here to fully characterize the viral pathogenesis and safety of our RABV/EBOV vaccine candidates in comparison to the live RABV vaccine that has been used extensively for wildlife vaccination in Europe.

Previous analysis of RV-GP and RVΔG-GP in immunocompetent mice demonstrated a complete lack of neuroinvasiveness upon intranasal, intraperitoneal, and intramuscular administration of virus demonstrating that expression of EBOV GP did not increase virulence of the RVA(p) (Blaney et al., 2011). Here, i.m. administration of RV-GP and RVΔG-GP to immunodeficient mice was utilized as an even more stringent assay for neuroinvasiveness. We demonstrated that RVA(p) and RVA retain a limited capacity to cause disease in immunodeficient mice. RV-GP also induced disease in one of eight immunodeficient mice. However, no mice inoculated with RVΔG-GP showed signs of disease indicating that it may have enhanced attenuation when compared to RVA(p), a recombinant derivative of the current live-attenuated wildlife RABV vaccine used in Europe.

Analysis of neurovirulence was conducted in adult and suckling immunocompetent mice. We demonstrated that RVA(p) is lethal in adult mice when administered by the i.c. route, but that RVA, a further attenuated vaccine vector containing an Arg→Glu change at amino acid 333 of RABV G, was avirulent under the same conditions as has been previously reported (McGettigan et al., 2003). Importantly, both RV-GP (derived from RVA) and RVΔG-GP showed no neurovirulence in adult mice. In contrast, we previously reported that both RVA and RV-GP retain neurovirulence in suckling mice analogous to RVA(p), while RVΔG-GP was found to be avirulent (Blaney et al., 2011). Here we confirmed that RVΔG-GP does not induce disease when administered i.c. to suckling mice and has at least a 19,000-fold reduction in neurovirulence when compared to RVA. In summary, our results in mice indicate that RV-GP (lack of neurovirulence in adult mice) and RVΔG-GP (lack of neurovirulence in adult and suckling mice) are both further attenuated for neurotropism than the current live RABV vaccine which has an excellent safety profile in Europe where millions of live-baited vaccines have been distributed.

In addition to the lack of neurovirulence observed for RVΔG-GP, the virus was shown not to proliferate in Vero cells; replication is restricted to the BSR-G *trans*-complementing cell line. Therefore, we sought to determine if the virus had any capability to replicate in the CNS. RVΔG-GP showed limited evidence of viral mRNA expression and/or genome amplification as assayed by RT-qPCR and production of infectious virus between days 7 and 14 which could only be detected on BSR-G cells. However, immunohistochemical analysis indicated that no morphologically detectable virus spread occurred as was readily observed for RVA. These results could suggest that upon i.c. inoculation, RVΔG-GP infected a small number of neurons or inflammatory cells mediated by the G present in virions followed by limited replication of the viral genome and production of virions which may contain residual G from the infecting RVΔGGP. However, the virus was unable to spread in the CNS because of the absence of additional expression of RV G. These results further support observations that RVΔG-GP has increased attenuation when compared to RVA(p) and should be pursued as a vaccine candidate.

The demonstration of attenuation of RV-GP and RVΔG-GP described here and the previous characterization of immunogenicity and protective efficacy in mice strongly support their consideration for use as wildlife vaccines. Both vaccine candidates induced strong humoral immunity to RABV and EBOV and conferred protection from RABV and MA-EBOV challenge in mice (Blaney et al., 2011). The ability of vaccination with RVΔG-GP to confer protection from RABV challenge indicates that the RABV G incorporated into the virions from the complementing cell line is sufficient to induce immunity to RABV. Use of these vaccine candidates in threatened NHP populations, which are highly susceptible to lethal EBOV outbreaks, could serve as a conservation success as field research over the past decade has indicated that lethal EBOV outbreaks have affected chimpanzee and particularly western gorilla populations in Gabon and the Democratic Republic of Congo (Bermejo et al., 2006; Le Gouar et al., 2009; Leroy et al., 2004; Vogel, 2006, 2007). With the successful history of vaccination of wildlife against RABV using dispersed baits containing the SAD B19 vaccine strain in Europe, one could consider using the live-attenuated RABV/EBOV vaccines in a similar manner in Africa. The introduction of SAD B19 RABV vaccine into Europe and safe dispersal of over 70 million vaccine baits since the 1980's provide a strong framework for this endeavor. Analysis of safety and immunogenicity of RV-GP and RVΔG-GP in NHPs administered oral vaccinations will be evaluated in the future. It is important to note that the interaction of humans and infected NHPs has been associated with transmission of EBOV to humans and initiation of subsequent outbreaks; therefore prevention of disease in NHPs may also serve to limit EBOV transmission into the human population.

Finally, it should be noted that although we are focused on the development of an inactivated RABV/EBOV vaccine for humans, RV-GP and particularly RVΔG-GP could be considered for use in humans as well. Live-attenuated vaccines are commonly associated with stronger T cell responses and more durable immunity, but the drawback of safety concerns in humans would be an issue requiring careful consideration. However, the growth restriction of RVΔG-GP and absence of neurovirulence in mice indicates that RABV vectored vaccines with a deletion in G, such as RVΔG-GP or an analogous, previously described human immunodeficiency virus vaccine candidate (Gomme et al., 2010), warrant further consideration for development as human vaccines.

Materials and Methods

Viruses

The recovery and propagation of the recombinant vaccine viruses used in this study have been described previously (Blaney et al., 2011; McGettigan et al., 2003). RVA(p) (rabies virus vaccine parent) serves as the parent rabies vaccine vector (previously termed BNSP) and is a recombinant virus derived from the SAD B19 RABV wildlife vaccine. RVA is a further attenuated derivative generated by introduction of a point mutation which results in an Arg→Glu change at amino acid 333 of RABV G (previously termed BNSP333). RV-GP was generated by introduction of EBOV Mayinga GP between the N and P gene of RVA. RVΔG-GP also expresses EBOV Mayinga GP but contains a deletion of the RABV G gene requiring propagation on *trans*-complementing BSR-G cells. BSR cells were originally derived from BHK-21 cells; BSR-G cells stably express RABV G upon induction with doxycycline (Gomme et al., 2010).

Viral growth curves

One-day old confluent 25 cm^2 flasks of Vero E6 or BSR-G cells were infected with vaccine viruses at an m.o.i. of 5 for a one-step growth curve or m.o.i. of 0.01 for a multi-step growth curve, respectively. Briefly, viruses were diluted in Cellgro Complete Serum free media (CCSFM, Mediatech), added to respective flasks, and incubated at 37°C, 5%CO2 for 1h.

Inocula were removed, and cells were washed 3x with PBS to remove unadsorbed virus. Five mls of CCSFM was added to each flask, and flasks were incubated at 37°C, 5%CO2. 100 μL of cell supernatants were removed at the indicated time points after infection. Samples were titered in duplicate using the respective cell lines on which they were grown as described previously (Gomme et al., 2010; Wirblich and Schnell, 2010).

Neuroinvasiveness in immunodeficient mice

All animal procedures described in this manuscript were conducted according to animal study protocols that were approved by the NIAID Institutional Animal Care and Use Committee. For analysis of neuroinvasiveness in immunodeficient mice, four to six week old female SCID mice (*ICRSC-F*; Taconic, Germantown, NY) were inoculated intramuscularly (i.m.) with either vehicle or $1x10^6$ FFU of vaccine viruses. Mice were counted and monitored for indications of encephalitis or other clinical signs daily. Moribund mice were euthanized immediately.

Neurovirulence

For evaluation of neurovirulence in adult mice, groups of eight four to five week-old female BALB/c mice were inoculated intracerebrally (i.c.) with either vehicle or 10^5 FFU of RVA(p), RVA, RV-GP, or RVΔG-GP. Mice were counted and monitored for indications of encephalitis or other clinical signs daily for four weeks. Moribund mice were euthanized immediately. For evaluation of neurovirulence in suckling mice, litters of 10 five-day-old Swiss Webster mice were inoculated i.c. with varying doses of RVA or RVΔG-GP as previously described (Blaney et al., 2011). Mice were counted and monitored for indications of encephalitis or other clinical signs daily for three weeks. Moribund mice were euthanized immediately.

The level of viral genomic RNA in suckling mouse brain was assayed by quantitative PCR. Five-day-old Swiss Webster mice were inoculated i.c. with $1x10^5$ FFU of RVA or RVΔGGP. On days 1, 3, 5, 7, 9, 14, and 21, three mice per group were sacrificed. Brains were removed and stored in RNAlater (Ambion) at 4°C until processing at which time they were weighed. RLT buffer (Qiagen) containing 10μl/ml of β-mercaptoethanol was then added to each brain to result in a 300mg/ml concentration, and brains were homogenized using a handheld homogenizer and disposable probes (Omni International). RNA was isolated from 30mg of each brain using an RNeasy kit (Qiagen), aliquotted and stored at -80°C until use. Reverse transcription was performed using a Transcriptor High Fidelity cDNA Synthesis Kit (Roche) with primer RP381 (5-ACA CCC CTA CAA TGG ATG C-3) for RABV N synthesis or 18S antisense primer (5-GGC CTC GAA AGA GTC CTG TA-3) for mouse 18S synthesis, which was used as a reference gene. Real-time PCR was performed on an ABI 7900HT Fast machine using a Dynamo Probe qPCR kit (Thermo Scientific) (Fig 5). The following primers and probes were used: mouse 18S rRNA sense primer (5-GGG GAA TCA GGG TTC GAT-3), mouse 18S rRNA antisense primer (5-GGC CTC GAA AGA GTC CTG TA-3), RABV N RNA sense primer (5-AGA AGG GAA TTG GGC TCT G-3), RABV N RNA antisense primer (5-TGT TTT GCC CGG ATA TTT TG-3), RABV N RNA probe (5-CGT CCT TAG TCG GTC TTC TCT TGA GTC TGT-3), and mouse 18S probe (5-CTG AGA AAC GGC TAC CAC ATC CAA GGA A-3). Custom primers and probes were purchased from Applied Biosystems.

For determination of infectious virus titers in suckling mouse brain, brain homogenates were collected and quantitated by focus forming assay. Briefly, five-day-old Swiss Webster mice were inoculated i.c. with $1x10^5$ FFU of the indicated virus. On days 1, 3, 5, 7, 9, 14, 21, 28, 35, and 42, three mice per group were sacrificed and brains were removed, immediately frozen on dry ice, and stored at -80°C. Brains were weighed and then homogenized in PBS

at 20% w/v using a hand-held homogenizer and disposable probes (Omni International). Samples were centrifuged at 1000xg for 10min, and supernatants were collected. The level of infectious virus in supernatants was determined by focus-forming assay on Vero cells or BSR-G cells as previously described (Gomme et al., 2010; Wirblich and Schnell, 2010).

Histopathology and Immunohistochemistry

Five-day-old Swiss Webster mice were inoculated i.c. with $1x10^5$ FFU of RVA or RVΔG-GP. On days 1, 3, 5, 7, 9, 14, and 21, three mice per group were sacrificed and brains were removed from the cranium, immersion-fixed in Bouin's solution for 24 hours, post-fixed in 70% isopropranol for 24–48 hours, processed according to standard protocols, and embedded in paraffin. Two 4-μm sections were obtained at the level of the hippocampus and at the level of the cerebellum. One section from each area was stained with hematoxylin and eosin (H&E) according to standard protocols. Immunohistochemistry was performed on the second section from each area. Sections first underwent heat-induced epitope retrieval (Biocare Rodent Decloaker, 10X, Biocare Medical, Concord, CA) for 15 minutes at 95°C, followed by incubation with a biotinylated mouse anti-RABV nucleoprotein monoclonal antibody (1:50; MAB8724, Millipore, Temecula, CA) for 12 hours at 4°C. Primary antibody was localized with horseradish peroxidase and diaminobenzidine substrate followed by hematoxylin counterstain. Negative control slides were handled identically except that non-immune serum was used in place of the primary antibody. All slides were randomized, blinded, and examined by light microscopy by a board-certified veterinary pathologist. Inflammation and immunohistochemical staining were semi-quantitatively scored on a 0–3 scale (0 = none, 1 = mild, 2 = moderate, 3 = severe).

Acknowledgments

These studies were supported in part by the NIAID Division of Intramural Research. We thank Nicholas Oberlander for contribution to the animal studies and Fabian de Kok-Mercado for assistance in preparation of figures.

References

Bermejo M, Rodriguez-Teijeiro JD, Illera G, Barroso A, Vila C, Walsh PD. Ebola outbreak killed 5000 gorillas. Science. 2006; 314:1564. [PubMed: 17158318]

Blaney JE, Wirblich C, Papaneri AB, Johnson RF, Myers CJ, Juelich TL, Holbrook MR, Freiberg AN, Bernbaum JG, Jahrling PB, Paragas J, Schnell MJ. Inactivated or live-attenuated bivalent vaccines that confer protection against rabies and Ebola viruses. Journal of virology. 2011; 85:10605–10616. [PubMed: 21849459]

Bradfute SB, Dye JM Jr, Bavari S. Filovirus vaccines. Hum Vaccin. 2011; 7:701–711. [PubMed: 21519188]

Bukreyev AA, Dinapoli JM, Yang L, Murphy BR, Collins PL. Mucosal parainfluenza virus-vectored vaccine against Ebola virus replicates in the respiratory tract of vector-immune monkeys and is immunogenic. Virology. 2010; 399:290–298. [PubMed: 20129638]

Cleaveland S, Fevre EM, Kaare M, Coleman PG. Estimating human rabies mortality in the United Republic of Tanzania from dog bite injuries. Bull World Health Organ. 2002; 80:304–310. [PubMed: 12075367]

Faber M, Lamirande EW, Roberts A, Rice AB, Koprowski H, Dietzschold B, Schnell MJ. A single immunization with a rhabdovirus-based vector expressing severe acute respiratory syndrome coronavirus (SARS-CoV) S protein results in the production of high levels of SARS-CoV-neutralizing antibodies. J Gen Virol. 2005; 86:1435–1440. [PubMed: 15831955]

Faul EJ, Aye PP, Papaneri AB, Pahar B, McGettigan JP, Schiro F, Chervoneva I, Montefiori DC, Lackner AA, Schnell MJ. Rabies virus-based vaccines elicit neutralizing antibodies, poly-functional CD8+ T cell, and protect rhesus macaques from AIDS-like disease after SIV(mac251) challenge. Vaccine. 2009; 28:299–308. [PubMed: 19879223]

Geisbert TW, Bausch DG, Feldmann H. Prospects for immunisation against Marburg and Ebola viruses. Rev Med Virol. 2010; 20:344–357. [PubMed: 20658513]

Gomme EA, Faul EJ, Flomenberg P, McGettigan JP, Schnell MJ. Characterization of a single-cycle rabies virus-based vaccine vector. J Virol. 2010; 84:2820–2831. [PubMed: 20053743]

Gomme EA, Wanjalla CN, Wirblich C, Schnell MJ. Rabies virus as a research tool and viral vaccine vector. Advances in Virus Research. 2011

Hensley LE, Mulangu S, Asiedu C, Johnson J, Honko AN, Stanley D, Fabozzi G, Nichol ST, Ksiazek TG, Rollin PE, Wahl-Jensen V, Bailey M, Jahrling PB, Roederer M, Koup RA, Sullivan NJ. Demonstration of cross-protective vaccine immunity against an emerging pathogenic Ebolavirus Species. PLoS Pathog. 2010; 6:e1000904. [PubMed: 20502688]

Knobel DL, du Toit JT, Bingham J. Development of a bait and baiting system for delivery of oral rabies vaccine to free-ranging African wild dogs (Lycaon pictus). J Wildl Dis. 2002; 38:352–362. [PubMed: 12038135]

Le Gouar PJ, Vallet D, David L, Bermejo M, Gatti S, Levrero F, Petit EJ, Menard N. How Ebola impacts genetics of Western lowland gorilla populations. PLoS One. 2009; 4:e8375. [PubMed: 20020045]

Leroy EM, Rouquet P, Formenty P, Souquiere S, Kilbourne A, Froment JM, Bermejo M, Smit S, Karesh W, Swanepoel R, Zaki SR, Rollin PE. Multiple Ebola virus transmission events and rapid decline of central African wildlife. Science. 2004; 303:387–390. [PubMed: 14726594]

Mahanty S, Bray M. Pathogenesis of filoviral haemorrhagic fevers. Lancet Infect Dis. 2004; 4:487–498. [PubMed: 15288821]

McGettigan JP, Pomerantz RJ, Siler CA, McKenna PM, Foley HD, Dietzschold B, Schnell MJ. Second-generation rabies virus-based vaccine vectors expressing human immunodeficiency virus type 1 gag have greatly reduced pathogenicity but are highly immunogenic. J Virol. 2003; 77:237–244. [PubMed: 12477829]

Mebatsion T, Schnell MJ, Cox JH, Finke S, Conzelmann KK. Highly stable expression of a foreign gene from rabies virus vectors. Proc Natl Acad Sci U S A. 1996; 93:7310–7314. [PubMed: 8692989]

Mustafa W, Al-Saleem FH, Nasser Z, Olson RM, Mattis JA, Simpson LL, Schnell MJ. Immunization of mice with the non-toxic HC50 domain of botulinum neurotoxin presented by rabies virus particles induces a strong immune response affording protection against high-dose botulinum neurotoxin challenge. Vaccine. 2011; 29:4638–4645. [PubMed: 21549784]

Rouquet P, Froment JM, Bermejo M, Kilbourn A, Karesh W, Reed P, Kumulungui B, Yaba P, Delicat A, Rollin PE, Leroy EM. Wild animal mortality monitoring and human Ebola outbreaks, Gabon and Republic of Congo, 2001–2003. Emerg Infect Dis. 2005; 11:283–290. [PubMed: 15752448]

Sanchez, A.; Geisbert, TW.; Feldmann, H. Filoviridae: Marburg and Ebola viruses. In: Knipe, DM.; Howley, PM.; Griffin, DE., editors. Fields virology. 5th ed. Philadelphia, PA: Lippincott Williams & Wilkins; 2007. p. 1409-1448.

Schnell MJ, McGettigan JP, Wirblich C, Papaneri A. The cell biology of rabies virus: using stealth to reach the brain. Nat Rev Microbiol. 2010; 8:51–61. [PubMed: 19946287]

Siler CA, McGettigan JP, Dietzschold B, Herrine SK, Dubuisson J, Pomerantz RJ, Schnell MJ. Live and killed rhabdovirus-based vectors as potential hepatitis C vaccines. Virology. 2002; 292:24–34. [PubMed: 11878905]

Sun Y, Carrion R Jr, Ye L, Wen Z, Ro YT, Brasky K, Ticer AE, Schwegler EE, Patterson JL, Compans RW, Yang C. Protection against lethal challenge by Ebola virus-like particles produced in insect cells. Virology. 2009; 383:12–21. [PubMed: 18986663]

Vogel G. Ecology. Tracking Ebola's deadly march among wild apes. Science. 2006; 314:1522–1523. [PubMed: 17158293]

Vogel G. Conservation. Scientists say Ebola has pushed western gorillas to the brink. Science. 2007; 317:1484. [PubMed: 17872416]

Vos A, Neubert A, Aylan O, Schuster P, Pommerening E, Muller T, Chivatsi DC. An update on safety studies of SAD B19 rabies virus vaccine in target and non-target species. Epidemiol Infect. 1999; 123:165–175. [PubMed: 10487653]

Vos A, Pommerening E, Neubert L, Kachel S, Neubert A. Safety studies of the oral rabies vaccine SAD B19 in striped skunk (Mephitis mephitis). J Wildl Dis. 2002; 38:428–431. [PubMed: 12038143]

Warfield KL, Swenson DL, Olinger GG, Kalina WV, Aman MJ, Bavari S. Ebola virus-like particle-based vaccine protects nonhuman primates against lethal Ebola virus challenge. J Infect Dis. 2007; 196(Suppl 2):S430–S437. [PubMed: 17940980]

Wirblich C, Schnell MJ. Rabies virus glycoprotein expression levels are not critical for pathogenicity of RV. J Virol. 2010

Highlights

- We are developing bivalent, live and killed vaccines for rabies and Ebola virus
- RABV vaccines expressing EBOV GP are avirulent upon i.c. inoculation of adult mice
- Deletion of RABV G results in a complete lack of neurovirulence in suckling mice
- These bivalent, live vaccines have strong safety profiles in comparison to current vaccines

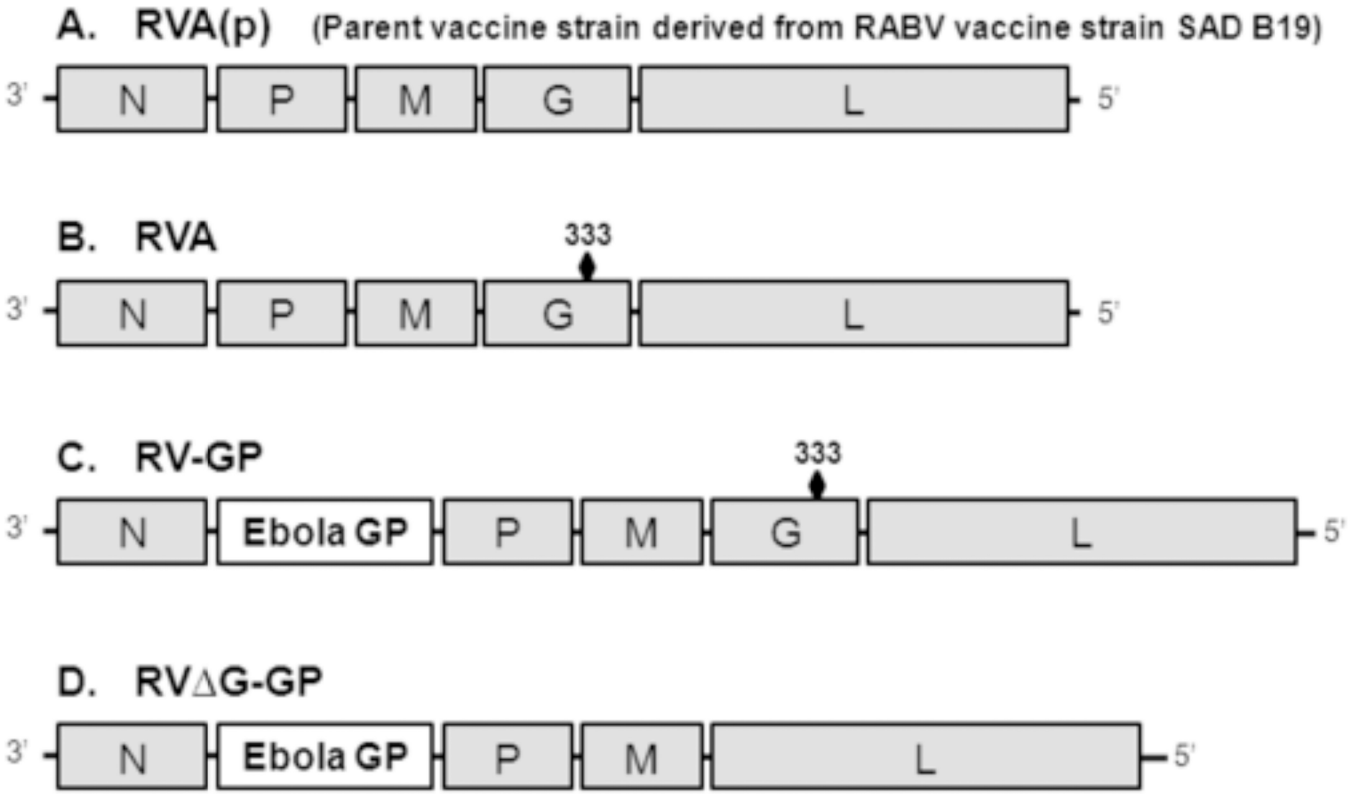

Figure 1.

Recombinant viruses. (A) Negative sense RNA genomes are illustrated for the parental rabies vaccine, RVA(p), which was previously termed BNSP. (B) The further attenuated derivative, RVA, contains an attenuating mutation at amino acid 333 of RABV G resulting in an Arg→Glu change, which restricts neurovirulence of RABV vaccines in adult mice. (C) RV-GP encodes EBOV Mayinga strain GP between RABV N and P from the RVA vector. (D) RVΔG-GP contains a deletion in the RABV G gene and is propagated on a complementing cell line, BSR-G cells, which express G.

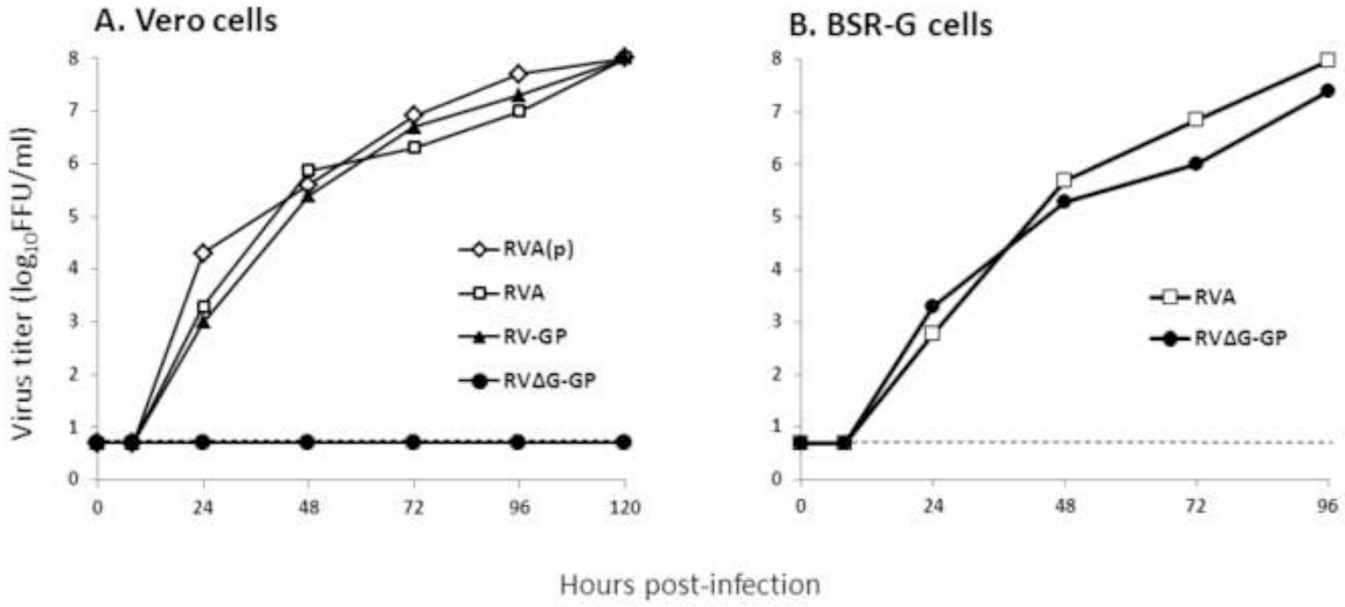

Figure 2.

Virus yields in cell culture. (A) Vero cells were infected with indicated viruses at an MOI of 5. BSR-G cells (a BHK cell derivative that expresses RABV G) were infected at an MOI of 0.01. Infected monolayers were incubated at 37°C for indicated time, and samples were removed for determination of virus yield. Virus concentrations were determined by viral focus assay. Dashed line indicates limit of detection.

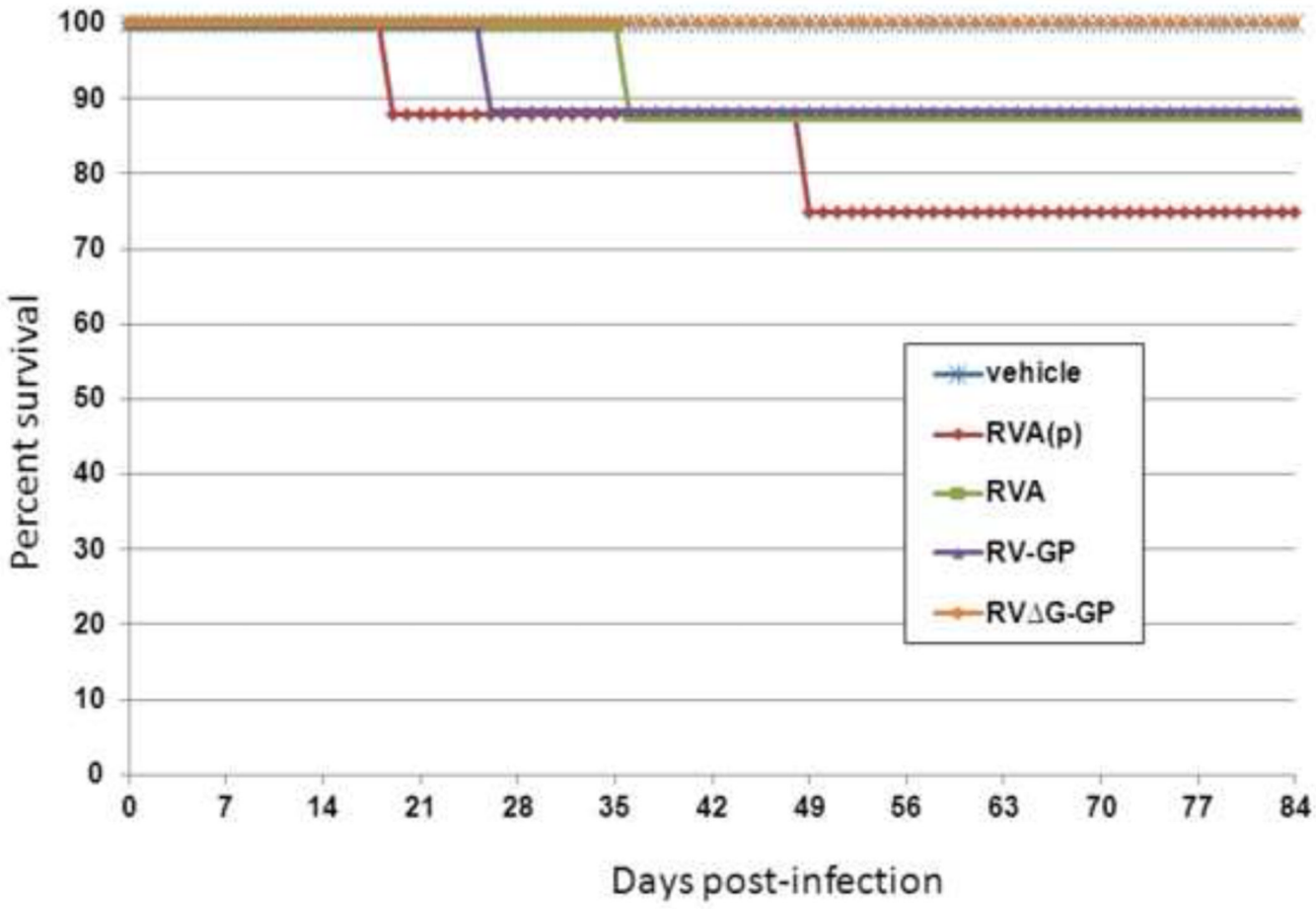

Figure 3.
Addition of GP to RVA does not increase neuroinvasiveness in immunodeficient mice. Groups of 8 4–6 week-old SCID mice were injected i.m. in the hind leg with $1x10^6$ FFU of the indicated virus and monitored daily for survival for 84 days.

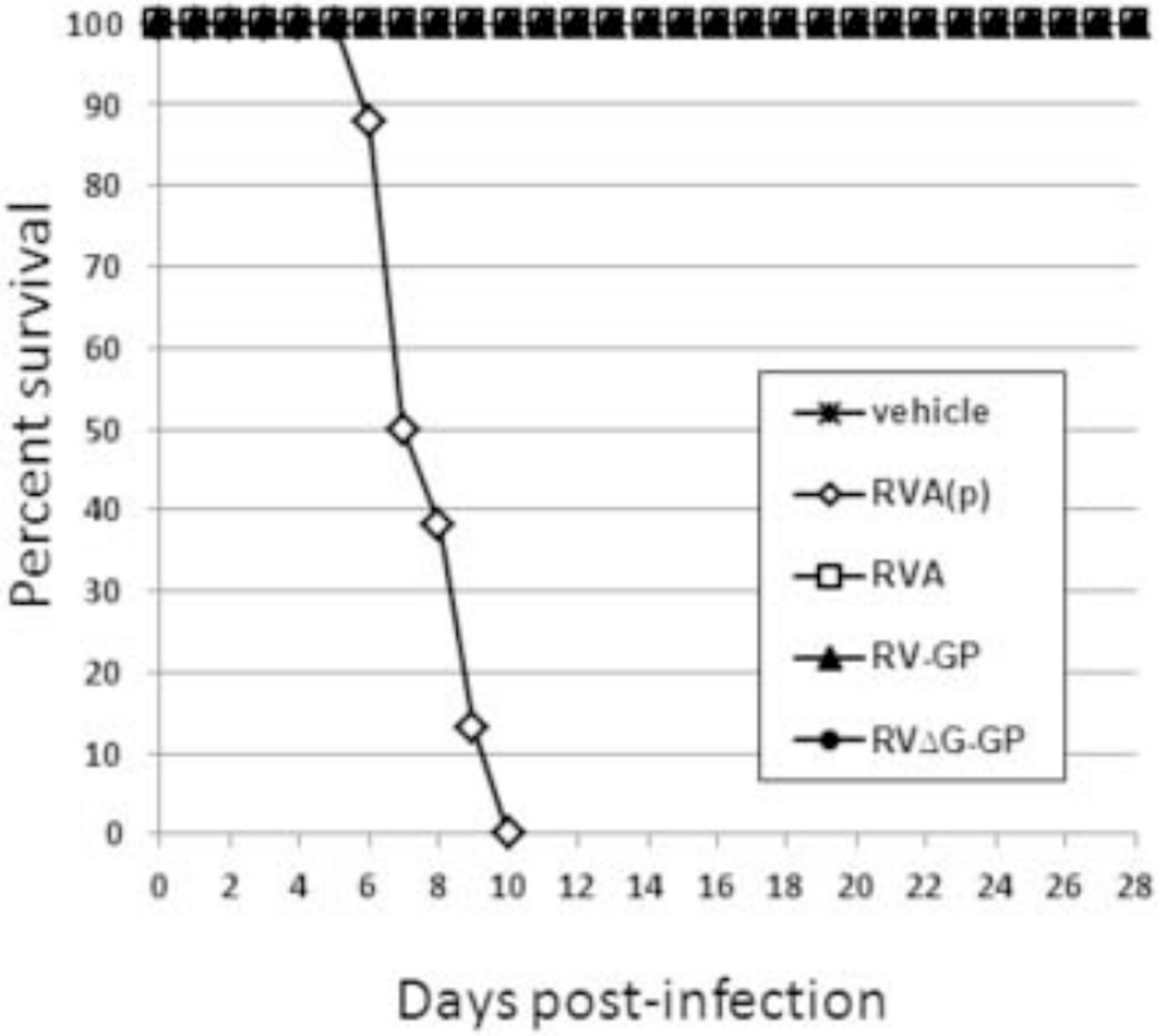

Figure 4.

RV-GP and RVΔG-GP are avirulent after intracerebral (i.c.) inoculation of adult mice. Groups of eight four week-old mice were injected i.c. with $1x10^5$ FFU of the indicated virus and monitored daily for survival for 28 days.

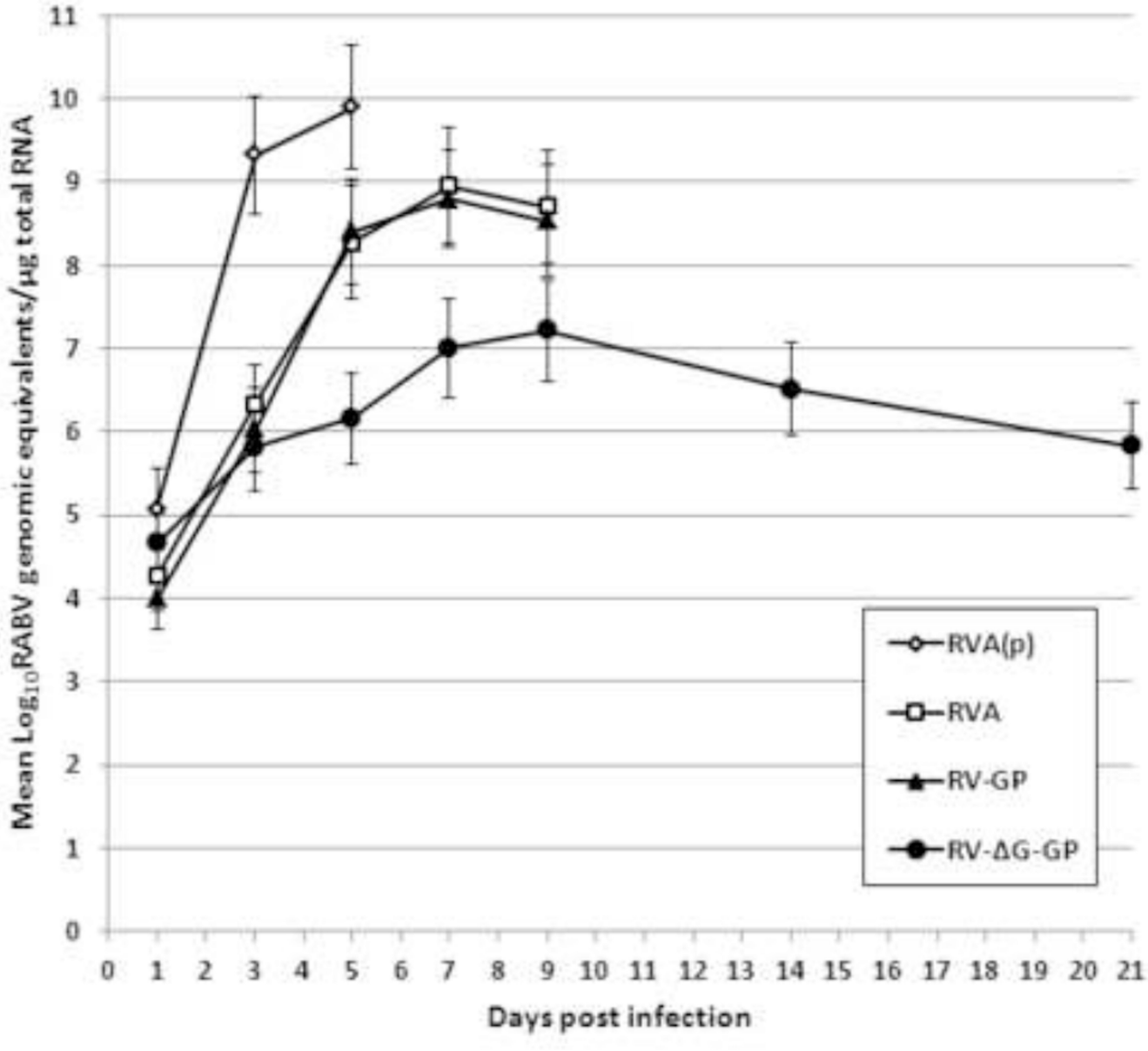

Figure 5.

Replication of vaccine candidates in suckling mouse brain assayed by quantitative PCR. Five-day-old Swiss Webster mice were inoculated i.c. with $1x10^5$ FFU of the indicated virus. On days 1, 3, 5, 7, 9, 14, and 21, three mice per group were sacrificed and brain homogenates were generated. The level of viral genomic RNA was determined by a RABV NPspecific quantitative RT-PCR assay.

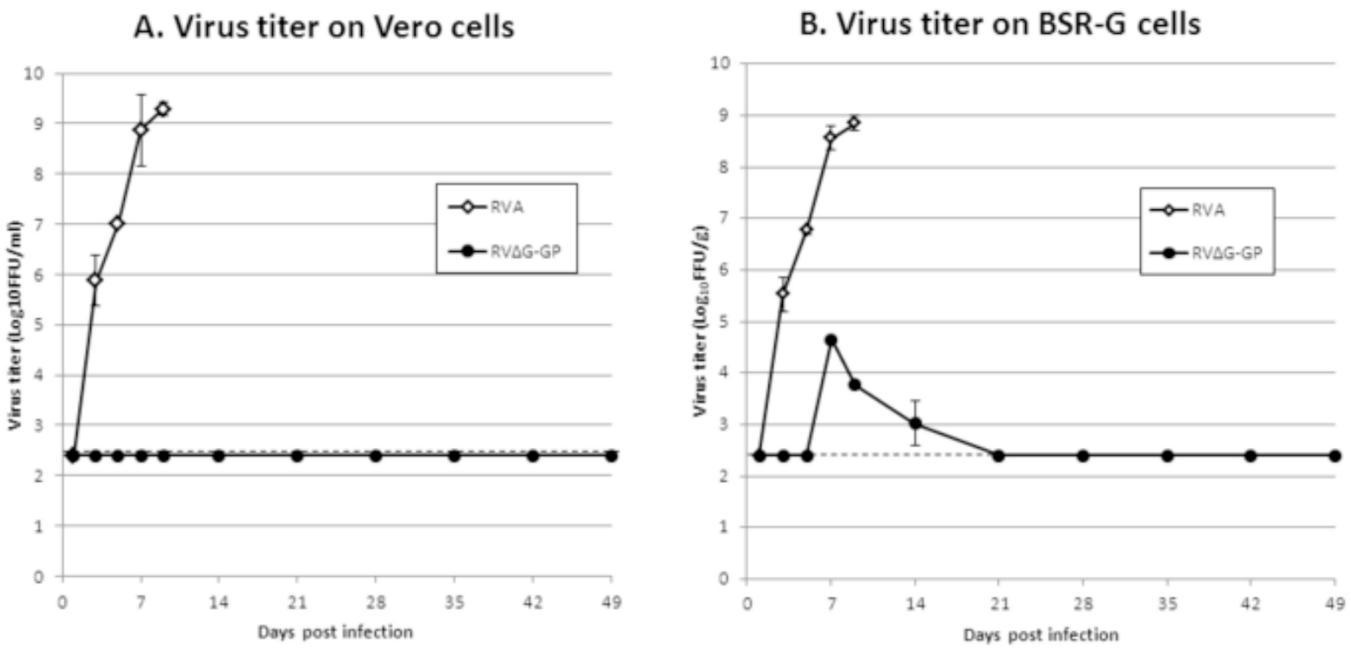

Figure 6.

Replication of RVΔG-GP in suckling mouse brain determined by virus focus assay. Five-day-old Swiss Webster mice were inoculated i.c. with $1x10^5$ FFU of the indicated virus. On days 1, 3, 5, 7, 9, 14, 21, 28, 35, and 42, three mice per group were sacrificed and brain homogenates were generated. The level of infectious virus was determined by focus-forming assay on (A) Vero cells or (B) BSR-G cells).

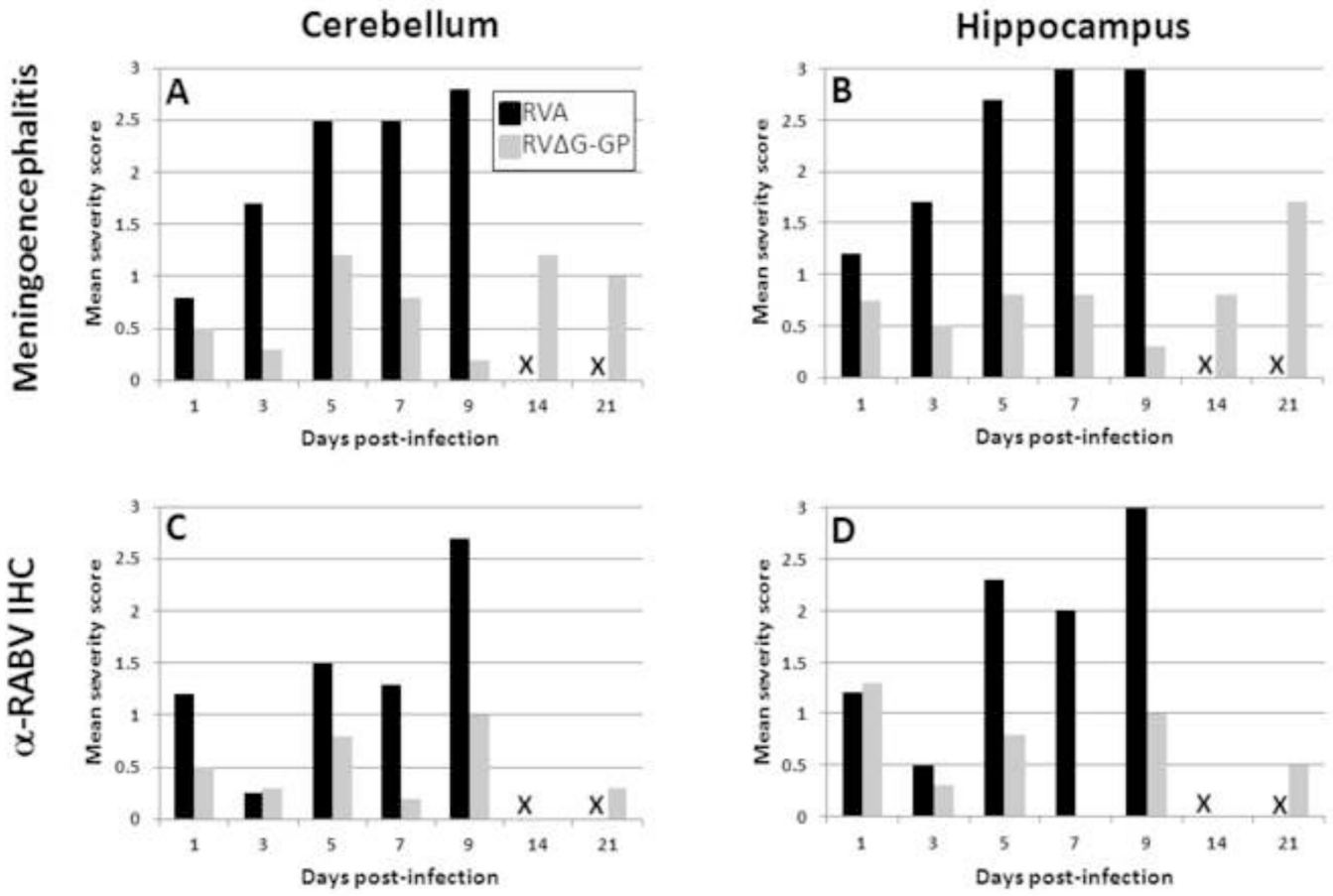

Figure 7.

Histopathological and immunohistochemical analysis of RVΔG-GP in suckling mouse brain. Five-day-old Swiss Webster mice were inoculated i.c. with $1x10^5$ FFU of the indicated virus. On days 1, 3, 5, 7, 9, 14, and 21, three mice per group were sacrificed and brains were processed for (A, B) H&E or (C, D) anti-RABV NP IHC analysis as described in the Materials and Methods. Inflammation and immunohistochemical staining were semi-quantitatively scored in the (A, C) cerebellum and (B, D) hippocampus in each of three brains per group using a 0–3 scale (0 = none, 1 = mild, 2 = moderate, and 3 = severe). The mean severity score is indicated. X indicates that all mice from the RVA group had succumbed to infection and were unavailable for analysis.

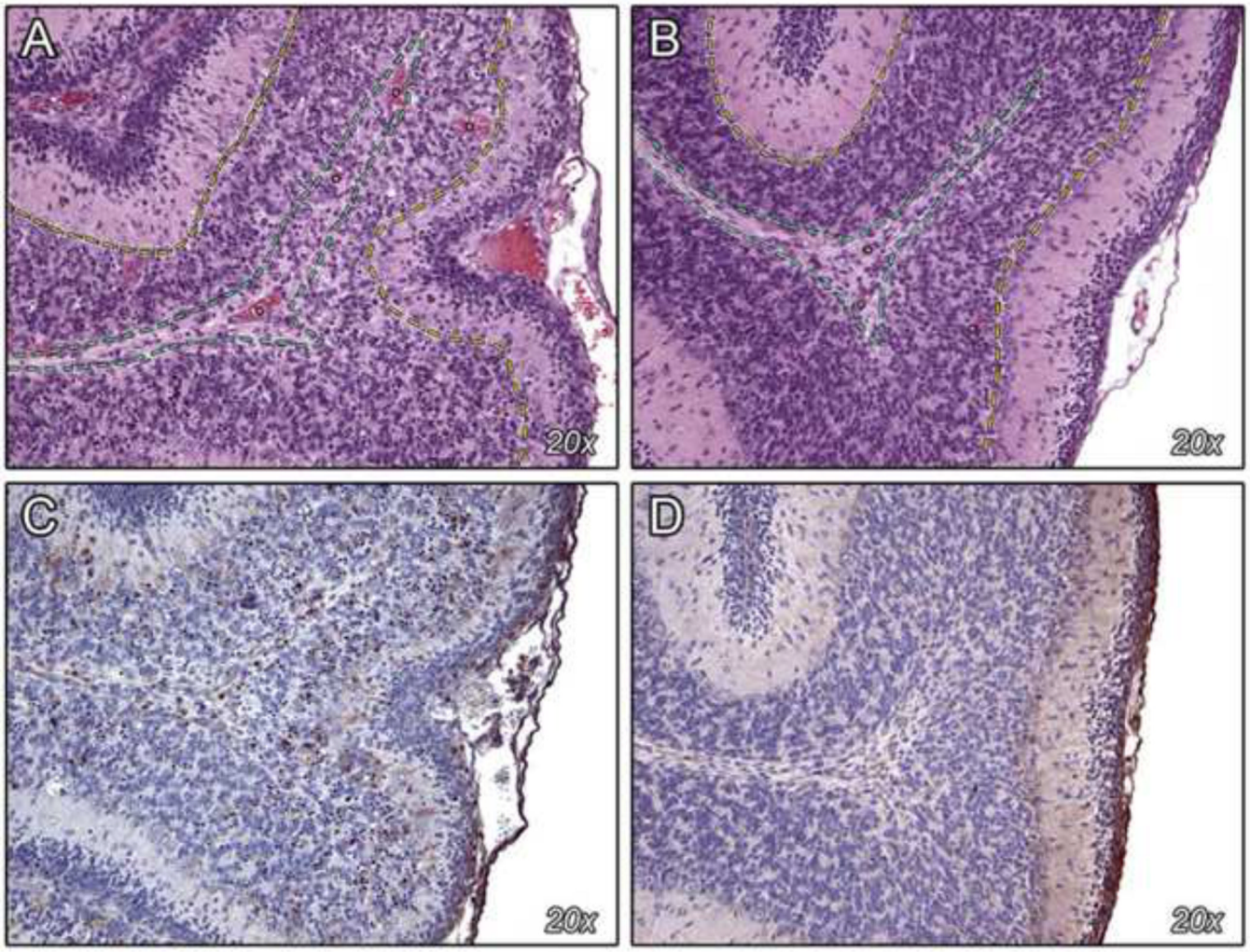

Figure 8.

Histopathology (H&E) and anti-RABV NP immunohistochemistry (IHC) of the cerebellum. Representative H&E (A, B) and IHC (C, D) of cerebellum from suckling mice inoculated i.c. with RVA (A, C) or RVΔG-GP (B, D). Size indicated is the objective magnification. A: Marked infiltration and disruption of the Purkinje cell layer (yellow dotted line) and granule cell layer (area between the yellow and green dotted lines), and to a lesser extent the molecular layer (pink area to the right of the yellow dotted line), by large numbers of neutrophils and lymphocytes. Also note dilatation and congestion of the capillaries (asterisks). B: Essentially normal cerebellum with well-delineated molecular, Purkinje, and granule cell layers, and normal capillaries (see A for explanation of annotations). C: Anti-RABV NP IHC showing numerous immunopositive (brown) neurons and inflammatory cells. D: Anti-RABV NP IHC showing minimal immunopositivity (brown).

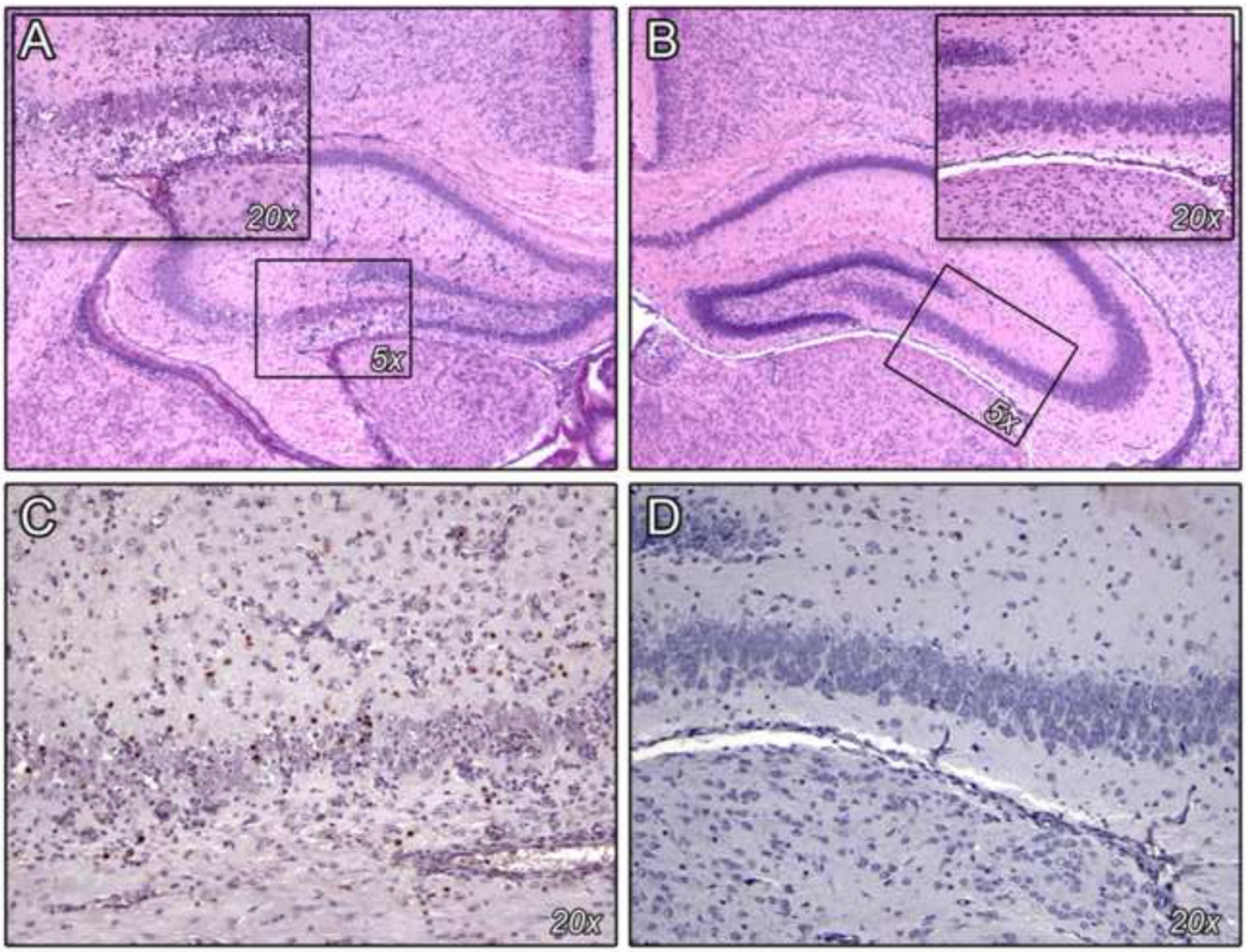

Figure 9.

Histopathology (H&E) and anti-RABV NP immunohistochemistry (IHC) of the hippocampus. Representative H&E (A, B) and IHC (C, D) of hippocampus from suckling mice inoculated i.c. with RVA (A, C) or RVΔG-GP (B, D). Size indicated is the objective magnification. A: Marked infiltration and disruption of the CA3-CA4 regions (boxed area) by neutrophils and lymphocytes. Also note rarefaction (paleness) of the surrounding neuropil and prominent capillaries lined by reactive endothelium. Inset shows higher magnification of the CA3-CA4 region containing large numbers of neutrophils, lymphocytes, and prominent capillaries. B: Essentially normal hippocampus. C: Anti-RABV NP IHC of the CA3-CA4 region showing large numbers of immunopositive (brown) inflammatory cells. D: Anti-RABV NP IHC of the CA3-CA4 region showing no significant immunopositivity (brown).

Table 1

RVΔG-GP (LD_{50} > 10^5 FFU) has at least a 19,000-fold reduction in neurovirulence when compared to the attenuated RVA (LD_{50} = 5.2 FFU) by i.c. injection of suckling mice.

Virus	Dose (FFU)	Survival[a] (%)	Mean day of endpoint (days± SE)
RVA	10^4	0	8.8 ± 0.3
	10^2	0	9.8 ± 0.4
	10^1	30	10.9 ± 0.4
	10^0	100	n/a
RVΔG-GP	10^5	100	n/a

[a]Five-day-old Swiss Webster mice (n=10) were inoculated IC with indicated dosage of virus and monitored for signs of encephalitis for 21 days.